**Fluorescence Correlation Spectroscopy as a Quantitative Tool Applied to Drug Delivery Model Systems**

C. C. Jung*, S. Polier, M. Schoeffel§, M. Drechsler, V. Jérôme, R. Freitag

University of Bayreuth, Universitätsstr. 30, 95447 Bayreuth, Germany

**Abstract**

The delivery of drugs to cells is a very active area of research. Drugs are commonly believed to ameliorate illnesses. The targeted, controlled and/or enhanced uptake of the drug into cells is facilitated by loading the drug into carrier vehicles (nanoparticles, e.g.. micelles).

The distribution of a drug over the nanoparticles used to deliver the drug to the targeted cells is of vital importance. It makes a difference, whether all nanoparticles carry the same amount of drug or whether a little amount of the nanoparticles carries a high proportion of the drug material and most nanoparticles carry no material. This depends on the method used to load the drugs into the carriers. Furthermore, the absolute amount of drug present in the nanoparticles and the absolute number of nanoparticles loaded with drug molecules is very important, because "dosis venum facit" [Paracelsus]. We present an approach to resolve these issues by optical means.

If the drug is fluorescent or labeled with a fluorescent label, fluorescence correlation spectroscopy (FCS) can be used to determine quantitative size distributions with a (confocal) microscope. In order to determine absolute concentrations the spatial dimensions of the confocal observation volume have to be known. These can be obtained from numerical simulations using vectorial diffraction theory. The theoretical results have been compared with experimental results from FCS using the calibration dye Rhodamine 6G. In a straightforward procedure the results were corrected for adsorption effects and excellent agreement to the theory was found.

Fluorescence correlation spectroscopy (FCS) and static and dynamic light scattering (SLS+DLS) were applied to determine quantitative loading distributions for diblock copolymer aggregates loaded with a fluorophore. These micelles were investigated as a model system for drug delivery. Poly(ethylene oxide)-*block*-poly(n-butyl acrylate) (PEO-*b*-PnBA) block copolymers of different molecular weights were synthesised and vesicles and micelles were prepared by drop-wise dilution, injection or dialysis. The aggregates were loaded with nile red or a perylene-bisimide derivative (PBI) either after the preparation or during the dialysis. Monomeric PBI molecules and aggregates of several PBI molecules were both found within the micelles.

The aggregates were applied to Chinese Hamster Ovarian (CHO) cells and the cells were investigated using flow cytometry, fluorescence microscopy and fluorescence microscopy spectroscopy. It was clearly demonstrated, that the block copolymer aggregates entered the CHO cells. It has to be stated that this particular block copolymer system is most probably not applicable to animals or humans because it is not biodegradable and was studied as a mere model system for the measuring method developed in this paper.

This measuring method has of course a very large application area for other (applicable) drug delivery systems.

**Introduction**

Drug delivery using self-assembled polymeric aggregates as nano-carriers is an active area of research. Here amphiphilic diblock copolymer micelles or so-called stealth nano-particles play a major role [T. Verecchia *et al.*, 1995]. For the application as drug delivery systems the hydrophilic block is chosen to be biocompatible and the hydrophobic part of the micelles forms a reservoir for a more hydrophobic drug [T. Trimaille *et al.*, 2006]. The micelles are taken up by the target cells by endocytosis and can release their content over a long time period or following a stimulus, like temperature, pH, ionic strength or light. The mean retention time within the cells is longer compared to low-molecular-weight (lmw) surfactants. The micelles are characterised by a high drug loading capacity, and a narrow size distribution. Their size can be tuned to facilitate their uptake by endocytosis. At the lower end the attainable size range comprises also the size of viruses.

Passive targeting of block copolymer micelles to cancer cells was reported in the literature [Y. Murakami *et al*., 1997 and *e. g.* L. L. Ma *et al*., 2008] and designated as the Enhanced Permeation and Retention (EPR) effect. An explanation lies in the defective vascular architecture of cancer cells due to their fast growth. Also vesicles or polymersomes have been successfully applied to tumors [D. E. Discher *et al*., 2007]. When considering this kind of therapy one always has to take into account, that the side-effect might be a cancerogenicity caused by the medical treatment itself.

The hydrophilic shell of the nano-containers serves two purposes: Firstly, the nano-containers are soluble in aqueous media. Secondly, if poly(ethylene oxide) is used as the hydrophilic part, the block copolymer aggregates are camouflaged [H. Otsuka *et al*., 2003 and M. Hamidi *et al*., 2006] and it is reported that the immune system does not recognise them [T. Verecchia *et al*., 1995 and S. M. Moghimi *et al*., 2001]. Diblock copolymer micelles also offer the perspective to be used in Photodynamic Therapy [B. H. Li *et al*., 2007]. An advantage but also a possible disadvantage of block copolymers micelles in therapeutic use might be their low level of renal excretion [i.e. G. Gaucher *et al*., 2005], which leads to higher accumulation in the targeted cells but which might finally lead to accumulation in the body. That drugs delivered by micelles show a better accumulation in the targeted cells than in the rest of the body was shown in a photodynamic therapy experiment of rats [N. Nishiyama *et al.*, 2007], where the side effects were drastically reduced.

When the drug is replaced by an organic fluorophore or anorganic quantum dot this system can be studied as a model system in imaging using fluorescence microscopy. Our aim was to compare the results for the radii and concentrations obtained by Static and Dynamic Light Scattering and Fluorescence Correlation Spectroscopy in order to obtain information about the distribution over the micelles of the fluorophore as model for a hydrophobic drug. These findings were correlated to endocytosis experiments into mammalian cells, which also rely on fluorescence (flow cytometry and fluorescence microscopy).

The size of a fluorescent object is related to its diffusion constant via the Stokes-Einstein relation and can therefore be determined by investigation of the fluctuations of the intensity in a small observation volume, which are caused by diffusion of the fluorophore into and out of this volume. This is the underlying principle of FCS [D. Magde *et al.*, 1974; R. Rigler *et al.*, 1993]. The technique can be used to determine the sizes and concentrations of proteins [T. Waizenegger *et al.*, 2002], DNA molecules or micelles labelled covalently or non-covalently with a fluorophore [S. T. Hess *et al.*, 2002; P. Schwille and E. Haustein, 2002]. The results obtained with micellar systems [*e. g.* H. Zettl *et al*., 2005 and 2007] can be important for drug delivery research [S. M. Moghimi *et al.*, 2001], if the drug is fluorescently labelled or the fluorophore is used as a model for the drug [R. Savic *et al*., 2003 and S. Slomkowski *et al*., 2006] or if the drug itself is fluorescent [e. g. Z. L. Yang *et al*., 2008]. The information obtained by FCS from micelles can be related to Dynamic Light Scattering and Static Light Scattering results [R. Erhardt *et al*., 2001]. Also the critical micellar concentration can thereby be obtained [O. Colombani *et al*., 2007]. As the decay can be influenced at high excitation intensities by the triplet decay of the dye, a small dye molecule should be used in order to ensure a low inter-system crossing rate. For special dyes the situation can be further complicated by cis-trans isomerisation [e.g. W. G. J. H. M. van Sark *et al.*, 2000].

* Corresponding author: jung_christoph@yahoo.de

§ Current address: Laboratoire d'Optique et Biosciences CNRS UMR 7645 - Inserm U 696, Ecole Polytechnique, Route de Saclay, 91128 Palaiseau Cedex, France

In FCS the decay time of the autocorrelation function can only be converted to the diffusion constant with knowledge of the spatial dimensions of the confocal observation volume. The determination of the concentration from the amplitude of the autocorrelation also requires this prior knowledge. This is also true for Raster Image Correlation Spectroscopy (RICS) [C. M. Brown *et al.*, 2008] and concentration measurements performed under flow [S. Y. Chao *et al*., 2007]. The necessary information can be approached by simulations [H. Zettl *et al*., 2007], [J. Enderlein *et al*., 2005]. This study will use new kinds of simulations and perform concentration measurements with their help.

**Methods and Materials**

**Synthesis and Characterisation of the Diblock Copolymers.** The diblock copolymers were synthesised using the general scheme of ATRP (Atom Transfer Radical Polymerisation) (Scheme 1):

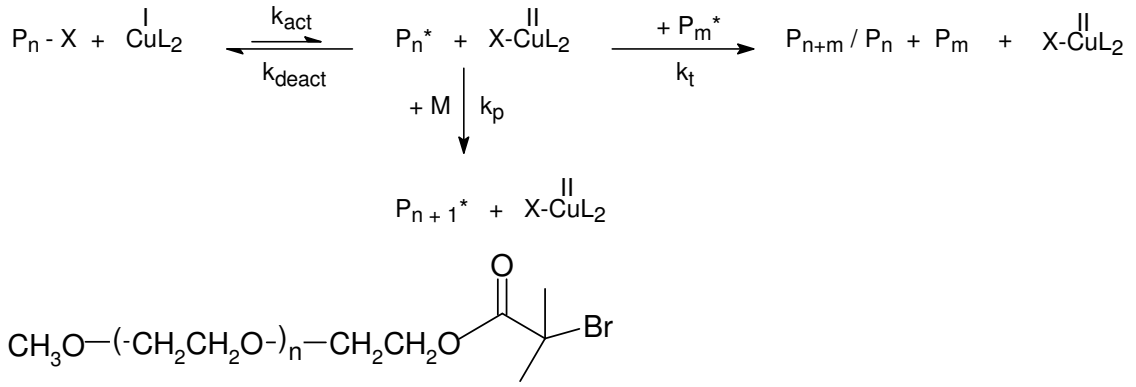


**Scheme 1**. Mechanism of ATRP and molecular formula of the macroinitiator PEO-Br.

PEO-Br was used as a macroinitiator (Scheme 1). The monomer M was n-butyl acrylate (nBA). 1, 14, 7, 10, 10-Hexamethyltriethylenetetramine (HMTETA) was used as the ligand $L_2$ for the CuBr catalyst. To tune the blocklength of the nBA block in the diblock copolymer the monomer/macroinitiator ratio as well as the reaction time (and therefore the percentage of conversion) were varied.

The resulting poly(ethylene oxide)-*block*-poly(n-butyl acrylate) (PEO-*b*-PnBA) diblock copolymers P1, P2 and P3 (Table 1) were characterised using Gel Permeation Chromatography (GPC) or Size Exclusion Chromatography, (SEC) and Proton Nuclear Magnetic Resonance ($^1$H-NMR). The lengths of the PnBA-blocks given in the sum formulae were determined by integration of $^1$H-NMR signals.

**Table 1.** Properties of the polymers to be used.

| Polymer | Monomer/ Macroinitiator ratio | Conversion | Polydispersity index (from RI data) | $M_w$ (GPC) in g/mol | Sum formula |
|---|---|---|---|---|---|
| P1 | 70:1 | 98 % | 1.24 | 13,400 | $PEO_{114}$-$PnBA_{64}$ |
| P2 | | 73% | 1.18 | 17,405 | $PEO_{114}$-$PnBA_{83}$ |
| P3 | 50:1 | 95% | 1.1 | 11,400 | $PEO_{120}$-$PnBA_{48}$ |

**Transmission Electron Microscopy.** For cryogenic transmission electron microscopy (cryo-TEM) studies, a drop of the sample was put on a lacey carbon transmission electron microscopy (TEM) grid, where most of the liquid was removed with blotting paper, leaving a thin film stretched over the lace. The specimens were instantly vitrified by rapid immersion into liquid ethane near its melting point in a temperature controlled freezing unit (Zeiss Cryobox, Zeiss NTS GmbH, Oberkochen, Germany). The temperature was monitored and kept constant in the chamber during all of the sample preparation steps. After freezing the specimens were inserted into a cryotransfer holder (CT3500, Gatan, München, Germany) and transferred to a Zeiss EM922 OMEGA EFTEM. Examinations were carried out at temperatures around 90 K. The transmission electron microscope was operated at an acceleration voltage of 200 kV. Zeroloss filtered images ($\Delta E$ = 0 eV) were taken under reduced dose conditions (100–1000 e/nm$^2$). All images were registered digitally by a bottom mounted CCD camera system (Ultrascan 1000, Gatan) combined and processed with a digital imaging processing system (Gatan Digital Micrograph 3.10 for GMS 1.5).

**Dynamic Light Scattering.** The measurements were performed at incidence angles between 30° and 150° using light scattering equipment with a hardware correlator (ALV-5000E, Langen, Germany) and a HeNe-laser as light source with a wavelength of 632.8 nm at temperatures of 20 °C, 25 °C and 37 °C. The light scattering cuvettes (Hellma, Germany) were cleaned using Piranha solution, immersed in water and washed in boiling distilled acetone. The solutions of the polymers were filtered using sterile filters (200 nm, PES, Supor Acrodisc, Pall).

**Fluorescence Correlation Spectroscopy (FCS).** FCS was measured on different home-built set-ups and on an Axiovert 100M with a Confocor2 unit (Zeiss, 40x magnification, C-Apochromat, NA=1.2, water immersion, variable cover glass correction; Long-pass-filter LP530, variable and non-variable attenuation filters) with an excitation wavelength of 488 nm. The home-built set-ups were characterised by simulation of the optical performance using vector diffraction theory and by measurements of a standard dye Rhodamine 6G (Merck, chloride salt). The objective used was an Olympus PlanApo 40x with an NA of 0.95 and a variable cover glass correction. An Argon ion laser was used at a wavelength of 488 nm and intensities below 100 µW. The fluorescence light was separated from the excitation light using one interference filter (either band pass from 525 nm to 725 nm or a long pass filter with a cut-off wavelength of 545 nm) and two color filters (OG515 and OG530, 3 mm, Schott, Mainz, Germany). Light detection was achieved by focusing the fluorescence light onto an avalanche photo-diode (50 µm rectangular aperture, PDM 50 ct from Micro Photon Devices, Bolzano, Italy). The data were collected using the PC card P7882 (FastComTec, Oberhaching, Germany) and software correlated to obtain the autocorrelation function. The normalization scheme was such, that for all delay times the squared average intensity of the whole run was used in the denominator of (1).

$$g_2(t) = \frac{\sum_\tau I(t) I(t+\tau)}{\left(\sum_\tau I(\tau)\right)^2} \quad (1)$$

**Labelling of nano-particles.** The nano-particles were labelled using Phenoxazone 9 (also called Nile red, Radiant Dyes Inc.) or N,N'-Di(1-heptyloctyl)-perylene-3,4:9,10-tetracarboxylic diimide (PBI, sample obtained from M. Thelakkat, University of Bayreuth) using

different methods described below (chemical structures see scheme 2). The quantum yield of PBI was determined by comparison to quinine sulphate and sulforhodamine 101 to 0.96 at room temperature in ethanolic solution.

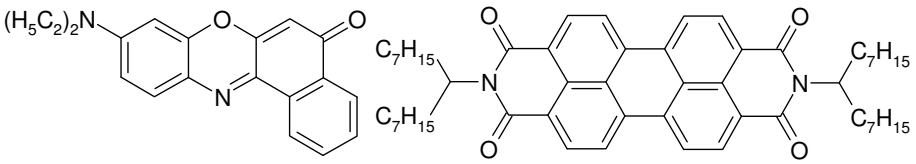

**Scheme 2.** Molecular formulae of Nile red (above) and of the non-covalent label PBI.

**Cell culture and endocytosis.** For all studies Chinese hamster ovary (CHO) cells were used. They were cultivated in RPMI 1640 medium (PAA Laboratories, Pasching, Austria), which was supplemented with 10 % fetal calf serum and 2 mM L-glutamine (PAA). Additionally, the medium contained 100 U penicillin and 100 µg/ml streptomycin (PAA). This complex medium will be referred to as medium below. Cells were incubated in a Thermo Forma Steri-Cult $CO_2$ Incubator HEPA-Class 100 (Thermo Forma, Marietta, Ohio, USA) at 37 °C, 90 % humidity and 5 % $CO_2$. The status of the cells was observed with the help of an inverted microscope (Olympus CKX41, Olympus, Tokyo, Japan).

All cell manipulation was done under sterile conditions in a laminar flow hood. First the culture medium was removed and the cells were washed twice with Dulbecco's PBS 1 (PAA) to remove traces of serum. 2×5 ml of PBS were used for a 10 cm tissue culture dish, 2×2 ml for each well of a 6-well plate. Then trypsin/EDTA (PAA) was added (1 ml for a 10 cm tissue culture dish, 0.5 ml for each well of a 6-well plate), cells were rinsed with the solution, and the excess was removed. Cells were exposed to trypsin/EDTA at room temperature for 5 min. The progress of the detachment was monitored by light microscopy. To inactivate the trypsin, the enzymatically detached cells were resuspended in serum containing medium.

Cell counting was performed according to the trypan blue method allowing for the distinction between viable and non-viable cells [J. R. Tennant, 1964]. 5 µl of a suitably diluted cell suspension were added to 45 µl of 0.4% trypan blue stain in PBS in a 96-well plate. The components were mixed thoroughly and incubated for 5 min at room temperature. 8 µl of this suspension were filled into a Neubauer counting chamber. Cells within a large square were counted by using an inverted microscope. One count per large square corresponds to $10^4$ cells/1 ml.

Cells were prepared for fluorescence microscopy and flow cytometry as follows. Cells from 10 cm cell culture plate were harvested and resuspended in 1 ml of medium. The cell number was determined using the trypan blue method. A suitable volume of the cell suspension was diluted with medium to a concentration of $10^5$ cells/ml. Then 2 ml aliquots were transferred to a 6-well plate. In contrast to plates used for flow cytometry, plates for microscopy were equipped with one coverslip per well. The plates were incubated overnight. Additionally, $10^5$ cells were plated on a 10 cm cell culture plate, diluted with 10 ml of medium and incubated for 2 d. This plate was used as a control in the FACS experiment.

**Endocytosis.** The incubation of the cells with micelles was started by replacing the medium from the 6-well plates (see 2.4) with 2 ml of fresh medium per well. Then a volume of medium which corresponded to the volume of the micelle or dye solution (N,N0-Di(1-heptyloctyl)-perylene-3,4:9,10-tetracarboxylic diimide (referred to as perylene below), doxorubicin or Nile red (scheme 2) which should be added was removed.

The solvent of the micelle or dye stock solutions was either water, PBS or RPMI 1640 depending on the experiment. Especially for incubation with larger volumes, an overnight dialysis of the aqueous micellar solutions against PBS or RPMI 1640 was carried out in order to reduce cell lysis. The micelles used in the different experiments varied in the following parameters: in the length of the hydrophobic part (PnBA), in the incorporated stain (no dye, perylene, doxorubicin or Nile red) and in the mode of the attachment of the dye (covalent or non-covalent).

Prior to the addition to the cells, all micelle or dye solutions were filtered using a Minisart 0.2 µm syringe filter (Sartorius, Göttingen, Germany). From these solutions, different volumina were added to the wells. Furthermore, for volumes of 500 µl, a volume of FCS corresponding to 10% of the volume of the micellar solution was added.

**Flow Cytometry.** After 24 h incubation of the CHO-K1 cells with micelles or free dye, cells were collected by trypsinisation. The inactivation of trypsin was performed using 1 ml of medium and the suspension was transferred to a 15 ml Falcon™ tube. The wells were rinsed with 1 ml of PBS each and the washing solutions were transferred to the corresponding tubes. The cells of the control plate were detached from the cell culture plate by washing with the medium present in the dish and the suspension was transferred to a 15 ml Falcon™ tube. All samples were centrifuged for 5 min at 1000 rpm and 4 °C in a Heraeus Multifuge 3 S-R (Heraeus, Berlin, Germany). Then most of the medium was removed and the cells were mechanically resuspended in the remaining medium. 1 ml of medium enriched with 1% (v/v) sytox green (stock solution: 10 µM in DMSO) was added to each tube. After 15 min incubation, the cell suspensions were centrifuged again (5 min, 1000 rpm, 4 °C). The supernatant was discarded, the cells were mechanically resuspended and 1 ml of PBS was added. The cell suspensions were poured into the FACS tubes and were analysed with the flow cytometer (Cytomics FC500, Beckmann Coulter, Krefeld, Germany). The threshold intensities for the discrimination between viable and non-viable cells (Sytox Green channel) and between cells containing or not dye-labelled micelles or free dye (Red channel) were determined by using the control sample.

**Fluorescence Microscopy**. After different incubation times, the CHO-K1 cells were prepared for fluorescence microscopy. The medium in the 6-well plates was removed and each well was washed twice with 2 ml of PBS. For fixation, 2 ml of a 4% paraformaldehyde solution in PBS were added to each well. After an incubation time of 10 min, the paraformaldehyde solution was removed and the coverslips were washed twice with bi-distilled water. The coverslips were incubated either in 1 ml of an aqueous 0.5 µM solution of Sytox Green for 10 min or in 2 ml of an aqueous 1 µg/ml solution of Hoechst 33258 for 20 min at room temperature. After staining, the coverslips were washed twice with bi-distilled water and stored in water until they were mounted in a drop of ProLong GoldTM antifade reagent (Invitrogen, Eugene, Oregon, USA) on a clean microscope slide. To prevent evaporation, the coverslips were sealed to the glass slide with clear fingernail polish.

The cells were observed under a fluorescence microscope (Olympus BX51, Olympus, Tokyo, Japan) equipped with a CCD camera (CC-12, Soft Imaging System, Münster, Germany) and Olympus U Plan FI objectives. The following filters were used for the detection of the fluorescence of the different dyes: Olympus NUA (excitation bandpass 360-370 nm, beam splitter 400 nm, emission filter 420-460 nm) for Hoechst 33258, Olympus NB (excitation bandpass 470-490 nm, beam splitter 500 nm, emission filter 520 nm) for Sytox Green, Olympus NG (excitation bandpass 530-550 nm, beam splitter 570 nm, emission filter 590 nm) for Nile red and PBI. The exposure times were chosen in order to obtain a good contrast ratio. All images were evaluated with the help of the computer program analySIS (Soft Imaging System, Münster, Germany).

**Fluorescence Microscopy Spectrometry.** Spectra in different regions of the microscope slides were recorded using a microscope combined with a spectrometer unit using a photomultiplier (MPV module from Leica, Wetzlar, Germany). The spectra were corrected for background fluorescence and for the wavelength dependence of the photomultiplier using a tungsten-halogen lamp with simultaneous current adjustment. The measurement was started, when the baseline such obtained was stable in the long wavelength region. The corresponding images were recorded on a microscope equipped with a color CCD camera (ColorView III, Soft Imaging System, Münster, Germany).

**Results and Discussion**

**An efficient way, to characterize a confocal set-up, using a new and simple expression for the point-spread-function.** The multiplication of the excitation intensity (which can be approximated by equation (2)) with the detection efficiency gives us the observation volume. This can be used to determine the autocorrelation function, which is expected for diffusion of a fluorophore through this confocal volume. In order to do this, we followed [S. T. Hess and W. W. Webb, 2002] with the exception, that we did not use the calculations of [Richards and Wolf, 1959], but instead used two different approaches to determine the point-spread function (PSF) expressed with our simple equations. Our new approach saves considerable computing time.

The point-spread-function of an optical system can be described using three parameters $w_x$, $w_y$ and $w_z$ and the formula depicted below, which follows from the energy conservation law and the observation, that I(0,0,z) can be fitted by a Gaussian, as well as I(x,0,0), I(0,y,0) and other cross-sections of I along the optical axis. This formula is new and we think it describes the situation better than previous ones.

$$I(x,y,z) = e^{-\frac{2z^2}{w_z^2}} e^{-\frac{2x^2}{w_x^2} e^{-\frac{2z^2}{w_z^2}}} e^{-\frac{-2y^2}{w_y^2} e^{-\frac{2z^2}{w_z^2}}} \tag{2}$$

Folding this point-spread-function (2) with a rectangular detector aperture with half-diameter a results in the detection efficiency (3).

$$D_a(x,y,z) = w_x \left( erf\left( \frac{\sqrt{2} e^{-\frac{z^2}{w_z^2}} (x-a)}{w_x} \right) - erf\left( \frac{\sqrt{2} e^{-\frac{z^2}{w_z^2}} (x+a)}{w_x} \right) \right) \cdot w_y \left( erf\left( \frac{\sqrt{2} e^{-\frac{z^2}{w_z^2}} (y-a)}{w_y} \right) - erf\left( \frac{\sqrt{2} e^{-\frac{z^2}{w_z^2}} (y+a)}{w_y} \right) \right), \tag{3}$$

where erf denotes the error function.

The first approach would be to take $w_x$, $w_y$ and $w_z$ from the literature [Cogswell and Larkin, 1995] and to assume an homogeneous illumination of the aperture, which is perfectly parallel to the optical axis. This approach leads within five minutes to a good result. The parallel illumination condition is satisfied in general. We have calculated that for our set-up the theoretical deviation from parallelity caused by Gaussian beams is in the pm-range and therefore not significant. However, the homogeneity of the beam is usually not given, this effect is commonly called apodisation, because it leads to the removal of the maxima near the main maximum in the focus. Also, of course $w_x$, $w_y$ and $w_z$ will depend on the aperture in a non-linear way for large apertures.

The second approach is to determine the confocal volume exactly. Therefore the radiation field at the focus of the objective was determined by integrating over the fields, which according to Huygens' principle originated from the far fields of the point dipoles distributed over the back aperture of the objective, whose intensities varied according to the Gaussian profile of the laser beam used to illuminate the objective. Here the polarisations of the dipole fields were taken into account using formula (4). Here $\vec{n}$ is the direction of the single beams connecting the point dipoles in the aperture plane with the point in the vicinity of the focus and $\vec{p}$ is the direction of the dipole in the aperture plane.

$$\vec{n} \times (\vec{n} \times \vec{p}) \tag{4}$$

The PSF for the detection was determined in a similar manner, but with equal intensities of the point dipoles over the whole back aperture and adding different emission wavelengths due to the Stokes' shifted emission spectrum. The spectral detection efficiency of the APD in comparison to the used fluorescence spectrometer also plays a role as well as the kind of long-pass filters used. Using relatively narrow band-pass filters this effect could possibly be diminished. However, the measured intensity would also be lower.

From these calculations (computing time: several hours) the parameters $w_x$, $w_y$ and $w_z$ (which are different for excitation and detection, respectively) were determined by fitting of a Gaussian to the functions I(x,0,0), I(0,y,0), I(0,0,z), and for the PSF, respectively.

The results of the two approaches are similar and therefore we suggest to follow the first approach in combination with our simple formulae (2), (3) and (4) in order to calculate the autocorrelation curve, which is expected for the respective set-up. We however followed the approach to use our own simulated confocal volumes and use the $w_x$, $w_y$ and $w_z$ extracted from the fits to Gaussians and inserted into formula (3).

This formula was used to determine the PSF in the approach described in [S. T. Hess and W. W. Webb, 2002], with the exception that we did also determine the number of the fluorescent particles (micelles) in the observation volume and not only their size.

**Experimental determination of concentrations and effective confocal volumes by FCS.** In order to be able to determine the effect of adsorption of the dye or micelle with dye to the cover glass on the apparent measured concentration of the fluorophores in the FCS experiment a straightforward procedure was adopted (Figs. 1 and 2). The fitting equation for FCS is equation (5).

A normal cover glass and a chambered cover glass with the same refractive index and similar thickness were used (e.g. Roth coverglasses and LabTek No.1 Borosilicate chambered coverslides, $n_D$=1.423 from Nunc). The small thickness variations can be corrected for using objectives with a variable cover glass thickness correction ring. In the following the different steps are described:

1. Take a 40 µl drop of the solution from a cuvette (determination of concentration as described below), place it on a normal cover glass and measure FCS.
2. Place a 40 µl drop of the solution whose concentration shall be determined on a normal cover glass and measure it.
3. Take a 40 µl drop from 2 ml of solution in a chambered cover glass, place it on an equivalent cover glass as used in 1 and measure FCS.
4. Do an FCS measurement of the solution directly in the chambered cover glass.

A 40 µl drop was found to give a constant value of the fluorescence intensity over a long time. This is due to a lucky cancellation of evaporation, photobleaching and long-distance diffusion because of adsorption.

The concentration in the cuvette and the concentration of an unknown solution were compared using the results from step 1 and step 2 (Fig. 1). The effective confocal volume and the percentage of adsorbed dye can be determined using the results from step 1, 3 and 4 (Figs. 1 and 2). The concentration in the 40 µl drop of the solution can then also be calculated and the effect of adsorption is eliminated.

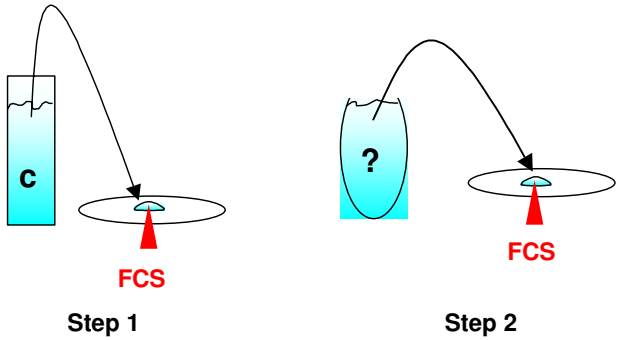


**Figure 1.** Schematic drawing of the experiments to determine the concentration of an unknown solution by FCS by comparison to a solution with known concentration

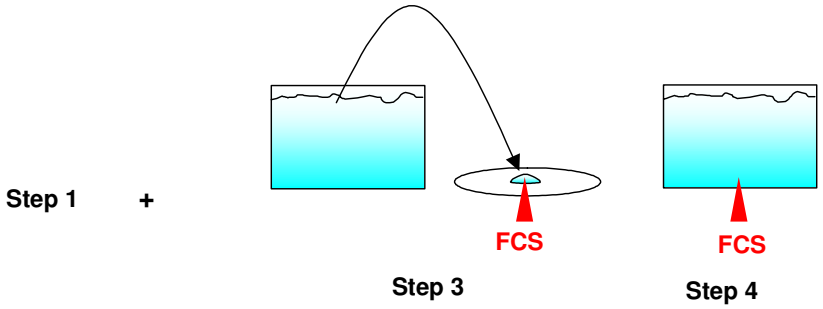


**Figure 2.** Determination of the effective volume using a normal cover glass and a chambered cover glass with similar n and d. After this step unknown solutions can be measured directly.

When using fluorophores with different emission spectra the effective confocal volume will be different from the values obtained using Rhodamine 6G or other calibration solutions because of a different point-spread-function for the detection. This effect is especially important when the detector aperture is overfilled.

**Determination of the concentration in the cuvette.** At low concentrations and high affinities of the fluorophore for the cuvette surface it is obvious, that adsorption will also change the concentration in the cuvette. The effect of adsorption is different in UV/Vis absorption spectroscopy and a fluorescence spectroscopy experiment. In the UV experiment the extinction of the adsorbed chromophores on the front and back faces of the cuvette is added to the measured spectrum. In the fluorescence experiment using a cuvette at right angle geometry, only the chromophores in the bulk of the solution are contributing to the measured fluorescence intensity.

Therefore the solution is measured in the same cuvette using both techniques. Then the solution is removed from the cuvette and the remaining adsorbed molecules are re-dissolved in the solvent used and the measurements using UV/Vis and fluorescence spectroscopy are repeated. If irreversible adsorption occurs, this can also be remedied by re-dissolving the adsorbed fraction in a small amount of a good solubilizing solvent and diluting this solution into the original solution.

The percentage of adsorbed particles or molecules can be determined by taking the ratio of the fluorescence spectra measured. The spectrum in the bulk of the cuvette can be determined by subtracting the two absorption spectra from each other.

Now the extinction coefficient of the solute is needed in order to compare the absorbance in the cuvette to the absorbance of a higher concentrated solution with known concentration. One can prepare this concentrated solution by precisely weighing out a known amount of the solute and dissolve it in a large beaker. The molecules adsorbed to the beaker walls are re-dissolved in the same solvent and re-measured. We have implicitly assumed that the aggregation of the chromophores in the solutions can be neglected. Therefore the linearity between absorbance and concentration should also be checked.

**Experimental Details.** The Rhodamine 6G concentration should be in the vicinity of 30 nM for the FCS experiments and the amount to be weighed out in order to prepare the concentrated solution should be higher than 2 mg. The extinction coefficient of Rhodamine 6G in the literature is given by 95 000 L/(mol·cm) in water, [D. Magde *et al.*, 1974]. The solutions in the cuvette and the chambered coverglass have to be shaken well and be protected from air and light.

**Corrected polarised emission spectra.** In order to theoretically determine the confocal volume it is necessary to know the corrected emission spectra of the fluorophores and the spectral quantum yield of the detector employed for fluorescence correlation spectroscopy. Here the issue of polarisation was taken into consideration for the corrected emission spectra.

First, the properties of the two identical polarisers were determined following the equations given in [C. C. Jung, 2004] with a UV/Vis absorbance spectrometer (Lambda 9, Perkin-Elmer). Then the polarisers were used to determine the characteristics of a more flexible lamp-monochromator-detector set-up. This set-up was then used to determine the polarised reflectivities at 45° incidence and reflection angle of a holographic diffuser (Varian), which in turn was used to determine the characteristics of a right angle fluorescence spectrometer (Cary Eclipse, Varian). Here the spectral characteristics of the excitation monochromator in the near-IR region were corrected for by determining the excitation spectra of a fluorescent solution of the dye IR-125 [R. C. Benson and H. A. Kues, 1977] with known absorption spectra. Then the corrected polarised emission spectra of the fluorescent solutions could be determined. Finally these spectra were multiplied with the spectral quantum yield of the detector unit of the FCS set-up and with the spectral characteristics of the long-pass filter used. These data were provided by the respective producers of the filters and the detector units of the FCS set-ups.

**Quantitative FCS. Calibration and measurement.** The results of the simulation using vectorial diffraction theory as shown in Table 2 have been compared to the experimental results from measurements performed with Rhodamine 6G in Table 3. Both experimental and theoretical decay curves were fitted to equation (5) in order to extract the parameters $w_0$ and $z_0$, which determine the confocal volume. D is the known diffusion constant of Rhodamine 6G [D. Magde *et al.*, 1974] and c is the concentration of the solution.

$$G(\tau) = 1 + \frac{1}{c\pi^{3/2} w_0^2 z_0 (1 + 4D\tau / z_0^2)} (1 + 4D\tau / z_0^2) \tag{5}$$

**Table 2.** Characteristics of three different home-built set-ups and one commercial set-up (Zeiss), as determined by vectorial diffraction theory (values are given for excitation wavelength of 488 nm, the PSF for the detection can be obtained by multiplication with the detection wavelength and division by 488 nm) and subsequent fitting of Gaussians.

| | | | Excitation | | Detection |
|---|---|---|---|---|---|
| Set-up | Apodisation [mm] | $w_x$ [nm] | $w_y$ [nm] | $w_z$ [nm] | Pinhole half diameter |
| I, excitation | 7.2 | 243 | 208 | 962 | 140.6 |
| II, excitation | 9.5 | 241 | 206 | 963 | 562.5 |
| III, excitation | 3.8 | 257 | 226 | 999 | 375 |
| PSF (I-III) | | 238 | 202 | 966 | |
| Excitation (Zeiss) | ∞ | 218 | 175 | 745 | 187.5 |

**Table 3.** Comparison of the parameters of equation (5) after fitting to the simulated decay curve (theory) and the experimental decay of the autocorrelation function (experiment). The parameter $z_0$ has been corrected for adsorption as described in the text.

| | **Theory** | | **Experiment** | | |
|---|---|---|---|---|---|
| | $w_0$ | $z_0$ | $w_0$ | $z_0$ | $z_0$ (ads.) |
| I | 203 | 1110 | 195 | | |
| II | 273 | 1665 | 295 | 1300 | 1640 |
| III | 268 | 1390 | 285 | 1000 | 1260 |
| Zeiss | 188 | 915 | 155 | 820 | 1000 |

The numbers clearly show the same trends for the experiments and the results of the simulation (Table 3). Excellent agreement is reached after correction for adsorption in the parameter $z_0$, which is necessary in order to determine the concentration of the solution. The recommended route to determine the concentration of a dye with unknown diffusion constant is therefore to first simulate the decay curve of the confocal set-up used and then use the parameters $w_0$ and $z_0$ such gained in the fit of the experimental results to equation (5) in order to extract D and the concentration c. Even concentration distributions over diffusion constants (or radii, see below) can then be determined, by using the program CONTIN from S. Provencher (see http://s-provencher.com/pages/contin.shtml). The diffusion constant in the case of the aggregates was converted to the hydrodynamic radius $R_h$ by using the Stokes-Einstein relation (equation (6)) with the viscosity $\eta$, the temperature T and the Boltzmann constant k.

$$D = \frac{kT}{6\pi\eta R_h} \tag{6}$$

**Preparation of nano-containers.** The preparation of the amphiphilic block copolymer aggregates involves first the dissolution in a so-called common solvent. That is a solvent, in which both blocks of the block copolymer are soluble. In such a solvent there is no aggregation tendency of the single polymer chains and these are completely dissolved.

In the second step this common solvent is slowly replaced by a solvent in which only one of the two blocks of the block copolymer is soluble. In such a solvent, be it hydrophilic, the hydrophilic block turns outwards from the formed aggregates and the hydrophobic blocks flee the solvent by sticking together in order to minimize the surface between them and the solvent. This process is similar to the folding of globular proteins.

There are several ways to accomplish this. One method is to prepare a very concentrated solution of the block copolymer in the common solvent and then slowly add the solvent, in which the aggregates are expected to form up to a quantity at which the percentage of the common solvent becomes negligible.

A solution of copolymer P2 was prepared in DMSO at a concentration of 10 mg/ml. A 25 µl drop of this solution was placed on the bottom of a glass beaker and 25 µl DMSO and then RPMI medium and serum were added drop-wise until 10 ml of the solution were produced. In Fig. 3 (DLS) and Fig. 4 (TEM) the resulting aggregates are depicted. The aggregates had a radius of 50 nm and were spherical, as there was no angular dependence in the light scattering results. The TEM pictures revealed the hollow structure of most of the aggregates. A bilayer formed the spherical shell and at the inside the aggregates were hollow and presumably filled with the same solution as outside. Such aggregates are commonly called vesicles

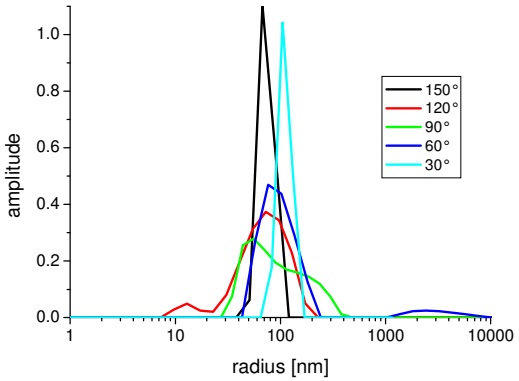


**Figure 3.** DLS of copolymer P2 (c=25 mg/ml) after drop wise addition of RPMI medium and fetal calf serum (with phenol red) to a DMSO solution. The temperature was 20 °C.

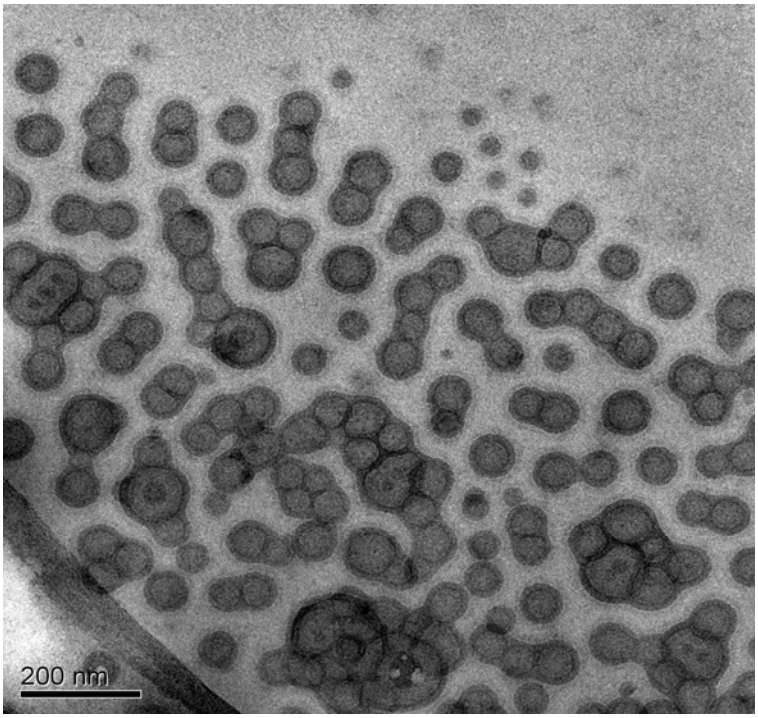


**Figure 4.** TEM micrograph of P2 vesicles prepared as described in Fig. 3.

Small spherical aggregates (radius 7.8 nm from DLS and 7.5 nm from FCS) resulted, when diluting from dioxane into dioxane/water (1:14)**.** This hints towards a micellar structure, because a bilayer in this case is not formed. In contrast, a core/shell structure is observed, where the core consists of the PnBA-block and the shell of the PEO-block. For comparison, the contour length of the block copolymer was 47 nm. This shows that we are not dealing with star-shaped micelles in this case.

**Preparation by dialysis.** Similar but larger micelles were formed, when the solution of a block copolymer in the common solvent was placed in a dialysis bag and this dialysis bag was placed into a mixture of dioxane and water (30:70). The solution outside of the dialysis bag was stepwise exchanged everyday for dioxane/water (50:50), dioxane/water (25:75) and three times pure water. The outside solution was changed daily.

When the hydrophobic fluorescent label is already present in the dialysis bag, it becomes incorporated into the copolymer aggregates. Figs. 5 and 6 (DLS and TEM) demonstrate the micellar nature of a solution such obtained. Two types of micelles can be observed: small spherical micelles with a radius around 20 nm and larger worm-like micelles

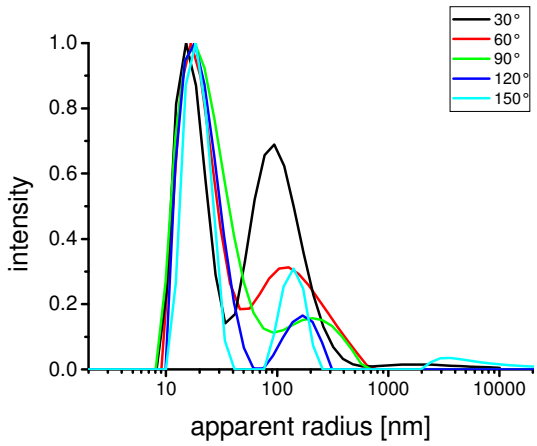


**Figure 5.** DLS (normalised) of micelles of copolymer P1 non-covalently labelled with PBI prepared by dialysis. For the SLS evaluation refractive index data from [Parker-TexLoc, 1997-2005] was used: $n_{PnBA}$=1.4740, $n_{PEO}$=1.4539.

.

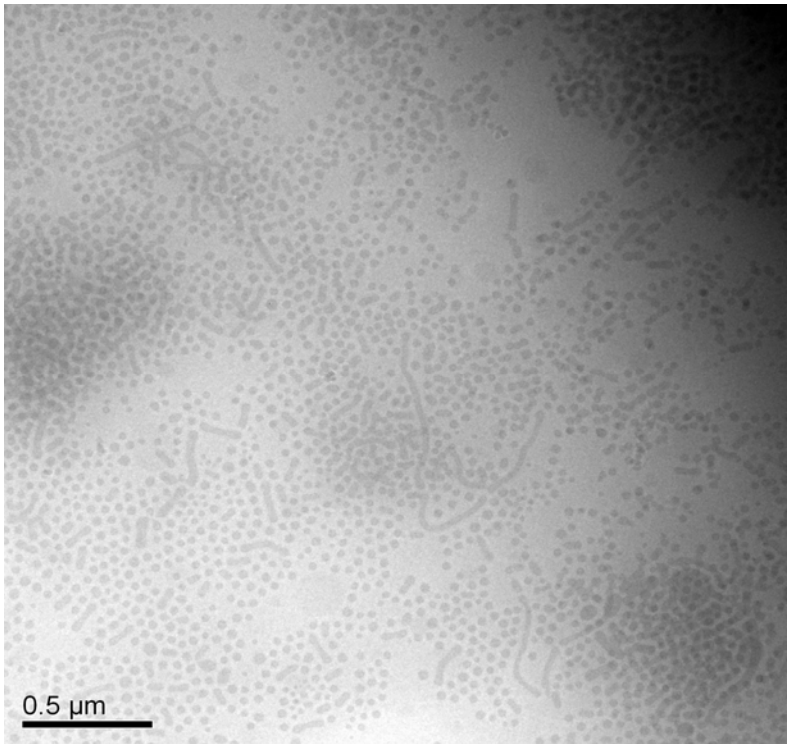


**Figure 6.** TEM micrograph of non-covalently labelled P1 micelles prepared by dialysis as in Fig. 5.

When an ethanolic solution of nile red (giving 408 nM nile red and 0.617 % ethanol) is added to the block copolymer solutions after the preparation of the block copolymer aggregates, FCS can be performed. In Figure 7 the autocorrelation curve of a vesicle solution is shown. The resulting radius is 71 nm, which is close to that found in the corresponding DLS experiment. Therefore fluorescence correlation spectroscopy can also be used to determine the size of block copolymer aggregates. The concentration, however, is grossly over-estimated, as can be judged by calculating the apparent molecular weight of such a vesicle. This may be due to the fact, that a high fraction of nile red is contained in the hydrophobic parts of the serum (probably in the proteins) and therefore reduces the FCS contrast, which results in too high an apparent concentration.

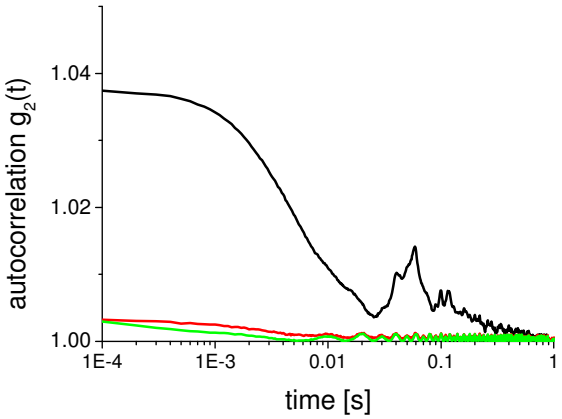


**Figure 7.** FCS in medium and serum of vesicles from copolymer P2 labelled with Nile Red. Red: Nile Red without vesicles. Green: Only medium and serum.

The results of FCS measurements of micelles prepared by dialysis of copolymer P2 in presence of PBI are shown in Fig. 8. The radius is 22.5 nm which is approximately the same as in the DLS experiment. However, the contrast was intensity dependent. This is expected, because the PBI aggregates are large emitting systems, which leads to a high intersystem-crossing rate, which in turn leads to a large triplet population and finally a large contribution of the triplet kinetics on the autocorrelation decay in relation to the signal from the PBI monomers [E. Lang *et al*., 2007]. In such a case only solutions labelled with the same chromophore and measured at the same excitation intensities can be compared with respect to their concentration and absolute concentrations and aggregate sizes can only be obtained by adjusting the excitation intensity. But sometimes even this is not possible. In the following experiments we used the excitation intensity, which lead to the maximum contrast. An example for the intensity dependence is shown in Fig. 9a. The apparent number of micelles in the confocal volume (inverse contrast) increases with increasing intensity because of the triplet decay becoming more important and increases for low intensities because of the increasing importance of the background fluorescence. A laser power around 10-20 nW gave the minimum values for the concentrations.

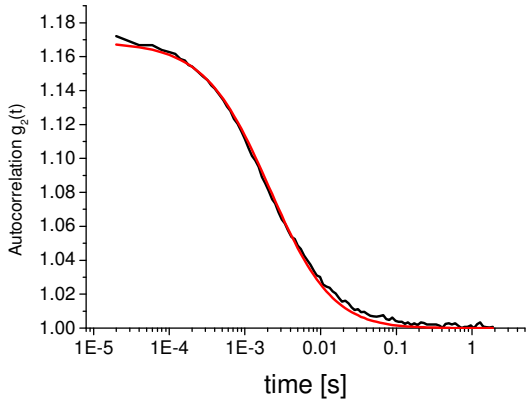


**Figure 8.** FCS of a solution of micelles of copolymer P1 (c=0.04 mg/ml) non-covalently labelled with PBI (OD of 0.01). Red: Fit with r = 22.5 nm and c = 21.7 nM.

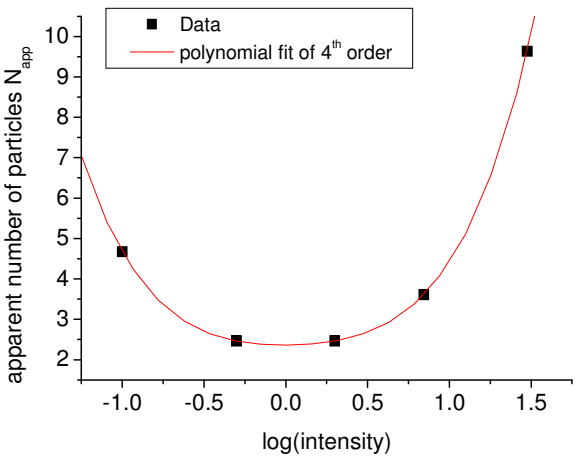


**Figure 9a.** Plot of the excitation intensity dependence of the observed apparent number of micelles in the FCS experiment using non-covalently PBI-labelled micelles. The minimum is observed at around 10-20 nW laser power in the focal plane.

In addition, as depicted in Fig. 9b, adsorption kinetics lead to a concentration varying in time in the con-focal observation volume in the vicinity of the cover-glass (50 µm distance). We used for the following experiments a distance larger than 200 µm from the cover-glass, where the concentration was not found to be time dependent during the measurement time.

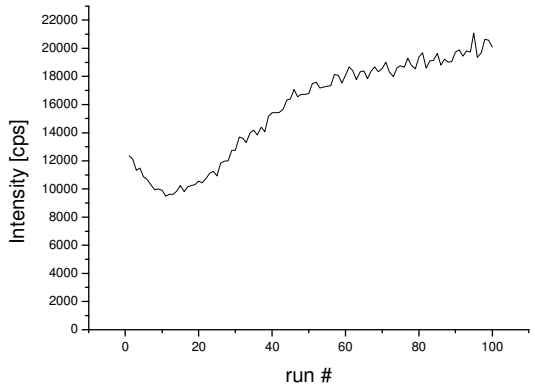


**Figure 9b.** Time dependence of the fluorescence intensity measured in 50 µm distance from the cover-glass in a solution of non-covalently labelled micelles of copolymer P1 (c=0.04 mg/ml).

We then compared the results of FCS and SLS measurements which were obtained with a time difference of less than 3 hours with FCS being measured first for a solution of copolymer P3 prepared by dialysis at a concentration of 0.5 mg/ml. The SLS gave a molecular weight $M_r$ of the micelles of 630 000 g/mol. The FCS gave a concentration of 538 nM and a fraction of adsorbed micelles of 50%, thereby resulting in a total concentration of 1.08 µM. The correction for the main emission wavelength gives 688 nM. If we combine the concentration of the micelles from FCS and the molecular weight of the micelles from SLS result the solution would have had c=0.41 mg/ml instead of the real c=0.5 mg/ml. If we compare the weighed-in concentration with the results from SLS combined to the result from FCS using the theoretical estimation for the Zeiss set-up used for this experiment the discrepancy is larger. The solution would have a concentration of 0.31 mg/ml instead of 0.5 mg/ml. It has to be stated, that the agreement is rather good. Obviously, not all of the micelles detected by DLS might have been labelled with fluorophores. However, the refractive index increment of the labelled micelles is higher than that of the unlabelled micelles, because of the Kramers-Kronig relations and therefore unlabelled micelles have less weight, which again should lead to a better agreement with the FCS experiment, where only the labelled micelles are detected. This slight discrepancy between FCS and DLS is the justification for doing this kind of measurements, because hints can be given, whether the loading procedure was capable to evenly distribute the fluorophores over the micelles (or the drugs over the carriers).

Figure 10 shows the determination of a distribution of the concentration of the micelles over the radii, determined using a CONTIN (S. Provencher) analysis applied to FCS.

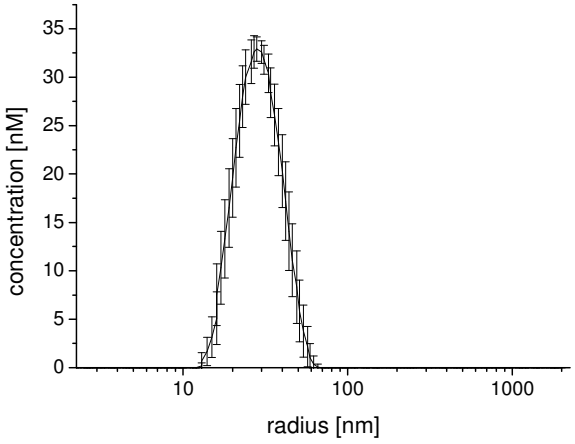


**Figure 10.** Distribution as determined by CONTIN analysis of the FCS results of a solution of P3 micelles (c=0.5 mg/ml) non-covalently labelled by PBI giving an $OD_{526\,nm}$ of 0.045.

Figure 11 shows AFM results of the same micellar solution of copolymer P3 diluted by a factor of 100 and placed on mica.

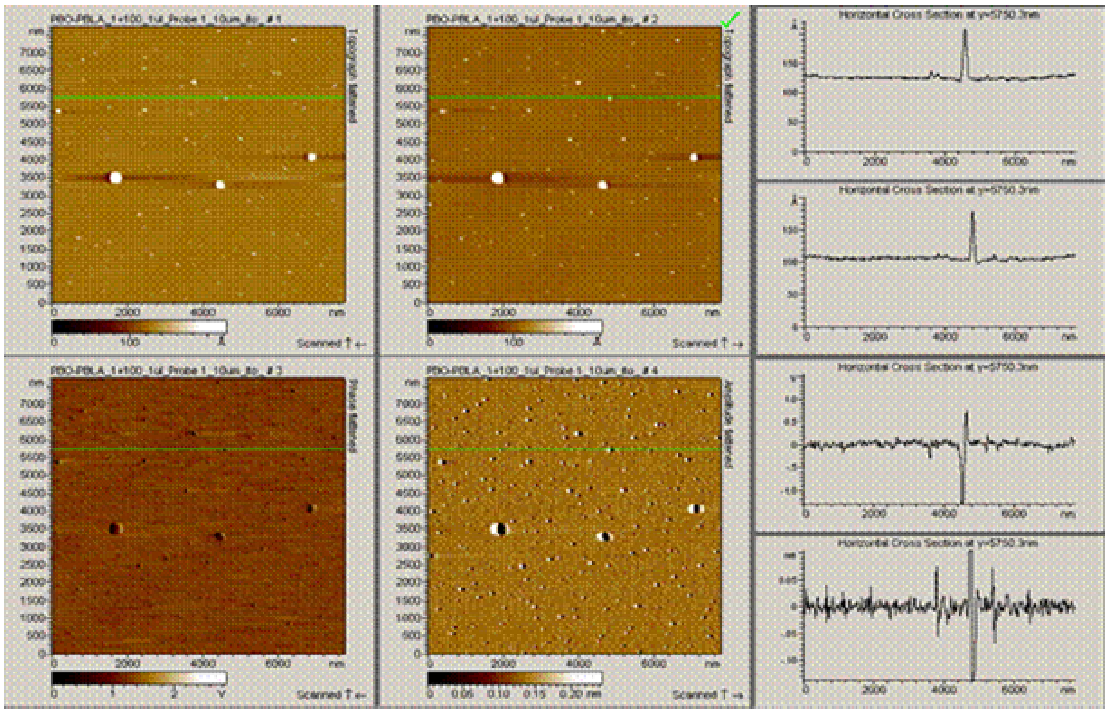

**Figure 11.** AFM images of drop of a 0.024 mg/ml solution of non-covalently labelled micelles of copolymer P3 placed on mica surface and left to evaporate.

**Endocytosis. Flow Cytometry, Fluorescence Microscopy, Fluorescence Microscopy Spectrometry (FMS).** Flow cytometry clearly demonstrates that the fluorescent PBI molecules could be delivered to the inside of the CHO cells by prior incorporation into the block copolymer micelles (Fig. 12). Obviously, PBI alone and the polymer alone did not label the cells to a significant extent. In the case of PBI this is due to the fact that the macroscopic aggregates of this insoluble compound were filtered out of the solution during sterilising by filtering through 200 nm filters.

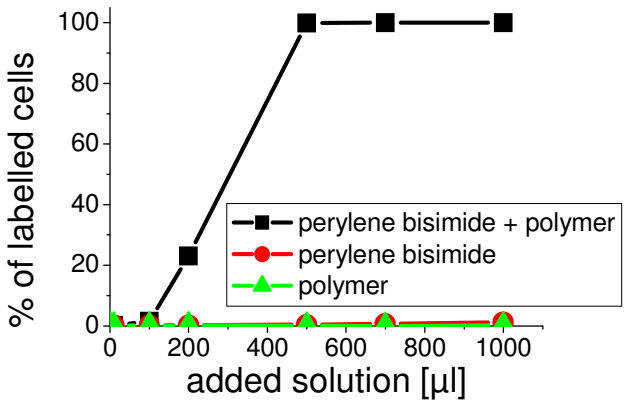


**Figure 12.** Effects on the addition of copolymer P1 micelles (c=2.4 mg/ml) non-covalently loaded with PBI to CHO-cells.

Absorption spectra in solution (Fig. 13), fluorescence emission spectra in solution (Fig. 14) and fluorescence microscopy spectrometry in the cells (Fig. 15) indicate that two different kinds of PBI forms prevail in the cells, as well as in the solutions. The blue shift of the absorbance spectrum (Fig. 13) could be attributed to the formation of H-aggregates (or "card pack" aggregates) of the dye molecules. The aggregated form of PBI however showed a long wavelength shifted emission spectrum (Fig. 14) compared to the non-aggregated dye.

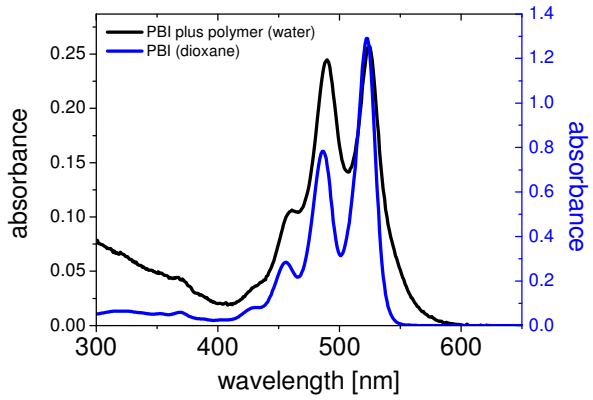


**Figure 13.** Absorption spectra of an aqueous solution of copolymer P1 micelles (c=2.4 mg/ml) non-covalently labelled with PBI.

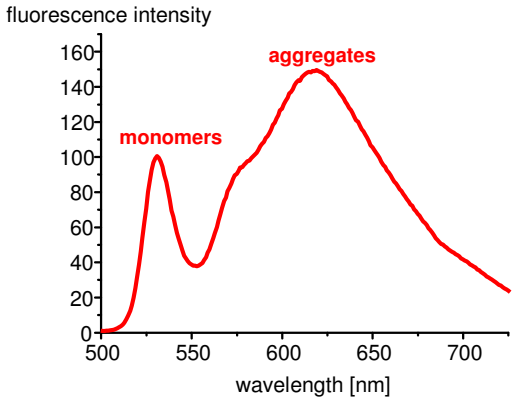


**Figure 14.** Fluorescence emission spectrum of copolymer P1 micelles (c=1 mg/ml) non-covalently labelled with PBI.

The two kinds of emitting species are also obvious from the coloured fluorescence microscopy experiments (Fig. 15). The squares in the images show the range, from which an emission spectrum was taken.

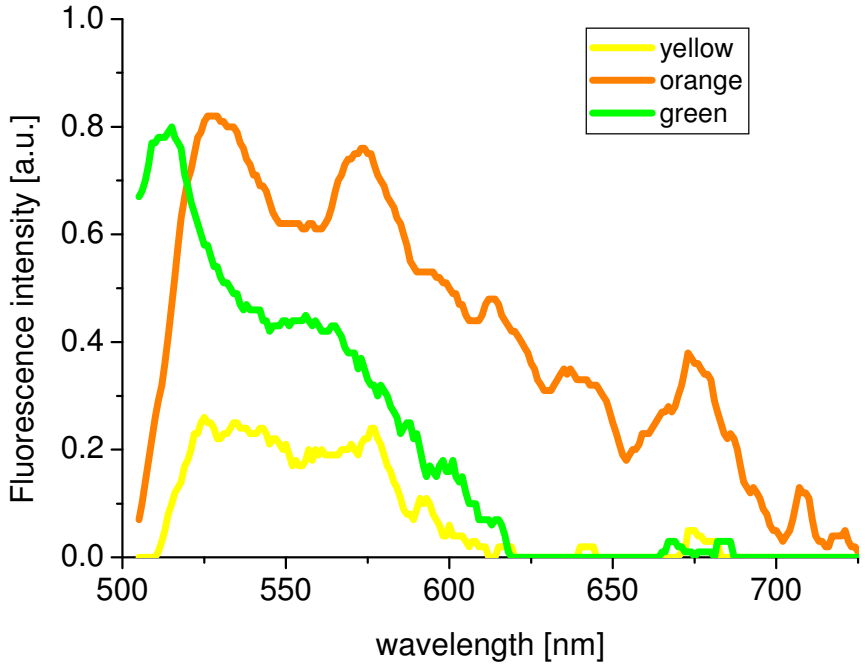
1.0
0.8
0.6
0.4
0.2
0.0
Fluorescence intensity [a.u.]
500
550
600
650
700
wavelength [nm]
yellow
orange
green

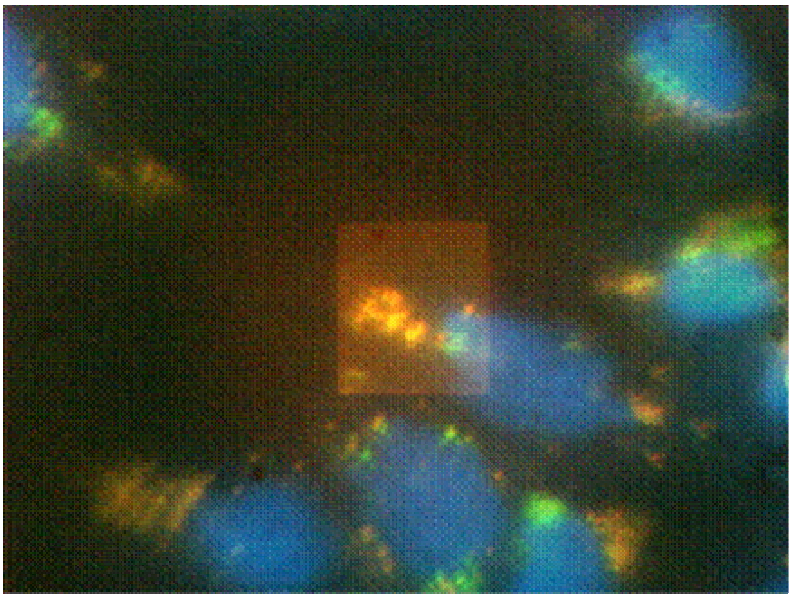

yellow

green

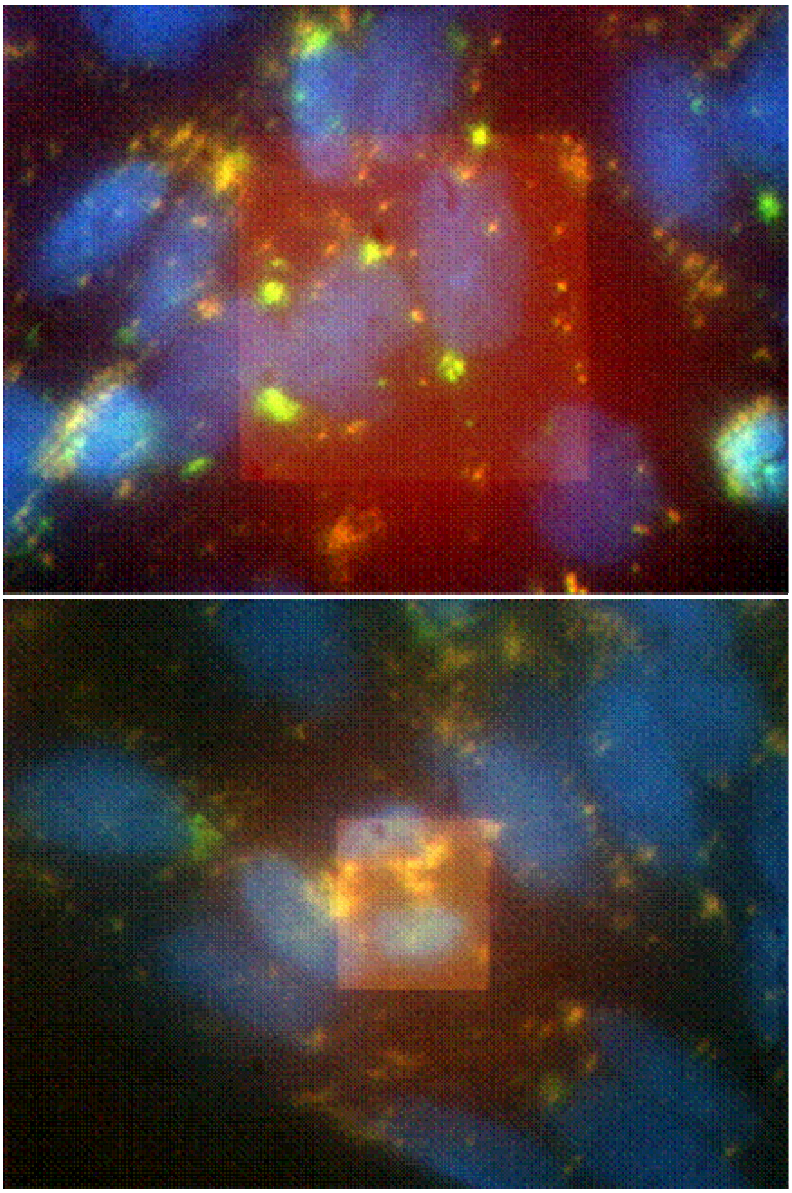

orange

**Figure 15**. Fluorescence microscopy spectrometry of CHO cells incubated with a solution of non-covalently labelled micelles of copolymer P1.

**Conclusions**

Furthermore FCS proved to be a powerful tool in combination with SLS and DLS to quantitatively compare different loading methods of nano-particles for the evenness of the distribution of the fluorophore over the nanoparticles (FCS and SLS) and to selectively characterise the properties of nano-particles, loaded with a fluorophore (DLS and FCS). The most efficient method to load the copolymer micelles with a fluorophore was to add the dye before the dialysis procedure for the preparation. Another, almost equally efficient or even better way is to dissolve the dye and the copolymer in a 10:1 acetone/water mixture and evaporating the acetone on a rotary evaporator. The advantage of the second procedure is the significantly reduced time requirement (roughly 2 hours instead of 7 days).

FCS was demonstrated to be a powerful tool in combination with theoretical simulations of the used confocal microscope to quantitatively determine diffusion constants and concentrations of unknown fluorescent molecules. The results of the experiment with the calibration dyes, especially of Rhodamine 6G, are significantly influenced by adsorption of the chromophore to the underlying cover glass. A straightforward procedure has been developed in order to correct for this effect and excellent agreement between the experimental and theoretical results was reached.

From the synthesised PEO-b-PnBA diblock copolymer three different kinds of aggregates could be prepared: vesicles and spherical star and crew-cut micelles. A small amount of worm-like micelles was also detected in the preparations containing the spherical star shaped micelles. The results from TEM, FCS and DLS are consistent with respect to these findings.

For the PBI-loaded micelles two different kinds of emitting species could be detected by fluorescence spectrometry. We attribute these species to micelles loaded with monomeric PBI units and micelles loaded with aggregated PBI units. The absorption spectrum compared well to reported spectra for aggregates of similar compounds [E. E. Neuteboom *et al.*, 2004]. Unfortunately, at the high intensities employed in most of the FCS experiments the triplet decay of this dye was the sole determining factor for the time constant of the FCS decay and therefore only estimates of the number of the micelle-dye aggregates could be obtained. When tuning the excitation intensity, such that a

maximum contrast (1/N) resulted from the fits to the FCS autocorrelation curves, a very good agreement between the concentrations determined from FCS and SLS was found.

The presence of two kinds of emitting species in the CHO cells could be confirmed using fluorescence microscopy and fluorescence microscopy spectrometry. Therefore the PEO-b-PnBA diblock copolymers synthesised by us can be effectively used to solubilise and deliver hydrophobic compounds to CHO cells. An attempt to show targeting was not made.

The dye nile red was small enough to avoid fast inter-system crossing, and could therefore successfully applied to discriminate aggregate sizes. The micelle-dye aggregates were taken up faster by the CHO cells than the nile red dye alone. For future experiments also the fluorescent coumarin dyes may also be usefool tools, because of their small size, which effects a long triplet decay time in the ms range. Also aggregation of the dyes within the block copolymer aggregates has to be prevented in order to be able to safely measure real concentrations.

**References**


0. Communication by Theophrastus Bombastus von Hohenheim, also called Paracelsus.
1. R. C. Benson and H. A. Kues, *J. Chem. Eng. Data* **22**, 379-383 (1977).
2. C. M. Brown, R. B. Dalal, B. Hebert, M. A. Digman, A. R. Horwitz, E. Gratton, *J. Microscopy* **229**, 78-91 (2008).
3. S. Y. Chao, Y. P. Ho, V. J. Bailey, T. H. Wang, *J. Fluoresc.* **17**, 767-774 (2007).
4. C. J. Cogswell, K. G. Larkin, in *Handbook of biological confocal microscopy*, J. B. Pawley, Ed. (Plenum Press, New York und London , ed. 2, 1995) chap. 8.
5. O. Colombani, M. Ruppel, F. Schubert, H. Zettl, D. V. Pergushov, A. H. E. Mueller, *Macromolecules* **40**, 4338-4350 (2007).
6. D. E. Discher, V. Ortiz, G. Srinivas, M. L. Klein, Y. Kim, C. A. David, S. S. Cai, P. Photos, F. Ahmed, *Prog. Pol. Sci*. **32**, 838-857 (2007).
7. J. Enderlein, I. Gregor, D. Patra, T. Dertinger, U. B. Kaupp, *ChemPhysChem* **6**, 2324-2336 (2005).
8. R. Erhardt, A. Böker, H. Zettl, H. Kaya, W. Pyckhout-Hintzen, G. Krausch, V. Abetz, A. H. E. Müller, *Macromolecules* **34**, 1069-1075 (2001).
9. G. Gaucher, M.-H. Dufresne, V. P. Sant, N. Kang, D. Maysinger and J.-C. Leroux, *J. of Controlled Release* **109**, 169-188 (2005).
10. M. Hamidi, A. Azadi, R. Rafiei, *Drug Delivery* 13, 399-409 (2006).
11. S. T. Hess and W. W. Webb, *Biophys. J.* **83**, 2300-2317 (2002).
12. C. C. Jung; "Lichtinduzierte Generierung und Charakterisierung optischer Anisotropie", (Dissertation, University of Potsdam, 2004).
13. E. Lang, R. Hildner, H. Engelke, P. Osswald, F. Würthner, J. Köhler, *ChemPhysChem* **8**, 1487-1496 (2007).
14. B. H. Li, E. H. Moriyama, F. G. Li, M. T. Jarvi, C. Allen, B. C. Wilson, *Photochem. Photobiol.* **83**, 1505-1512 (2007).
15. D. Magde, E. L. Elson and W. W. Webb, *Biopolymers* **13**, 29-61 (1974).
16. L. L. Ma, P. Jie, S. S. Venkatraman, *Adv. Funct. Mater*. **18**, 716-725 (2008).
17. S. M. Moghimi, A. C. Hunter and J. C. Murray, *Pharmacological Reviews* **53**, 283-318 (2001).
18. Y. Murakami, Y. Tabata, Y. Ikada, *Drug Delivery* **4**, 23-31 (1997).
19. E. E. Neuteboom, S. C. J. Meskers, E. W. Meijer, R. A. J. Janssen, *Macromol. Chem. Phys.* **205**, 217–222 (2004).
20. N. Nishiyama, W.-D. Jang and K. Kataoka, *New J. Chem*. **31**, 1074-1082 (2007).
21. H. Otsuka, Y. Nagasaki, K. Kataoka, *Adv. Drug Delivery Rev*. 55, 403-419 (2003).
22. Parker-TexLoc; "TexLoc Refractive Index of Polymers", http://www.texloc.com/closet/cl_refractiveindex.html (1997-2005).
23. R. Rigler, U. Mets, J. Widengren, and P. Kask, *Eur. Biophys. J. Biophys. Lett*. **22**, 169–175 (1993).
24. B. Richards and E. Wolf, *Proc. R. Soc. Lond. Ser. A.* **253**,358–379 (1959).
25. R. Savic, L. B. Luo, A. Eisenberg, D. Maysinger, *Science* **300**, 615-618 (2003).
26. P. Schwille and E. Haustein; „Fluorescence correlation spectroscopy. An introduction to its concepts and applications", http://www.biophysics.org/education/schwille.pdf, 2002.
27. S. Slomkowski, M. Gadzinowski, S. Sosnowski, I. Radomska-Galant, A. Pucci, C. DeVita, F. Ciardelli, *J. Nanosci. Nanotech.* **6**, 3242-3251 (2006).
28. J. R. Tennant, *Transplantation* **2**, 685-694 (1964).
29. T. Trimaille, K. Moudon, R. Gurny, M. Möller, *Int. J. Pharm.* **319**, 147-154 (2006).
30. W. G. J. H. M. van Sark, P. L. T. M. Frederix, D. J. van den Heuvel, M. A. H. Asselbergs, I. Senf and H. C. Gerritsen, *Single Mol.* 4, 291-298 (2000).
31. T. Verrecchia, G. Spenlehauer, D. V. Bazile, A. Murrybrelier, Y. Archimbaud, M. Veillard, *J. of Controlled Release* **36**, 49-61 (1995).
32. T. Waizenegger, R. Fischer, and R. Brock, *Biol. Chem.* **383**, 291-299 (2002).
33. Z. L. Yang, X. R. Li, K. W. Yang, Y. Liu, *J. Biomed. Mater. Res. A* **85**, 539-546 (2008).
34. H. Zettl, Y. Portnoy, M. Gottlob, G. Krausch, *J. Phys. Chem. B* **109**, 13397-13402 (2005).
35. H. Zettl, U. Zettl, G. Krausch, J. Enderlein, M. Ballauff, *Phys. Rev. E* **75**, 061804 (2007).



**Acknowledgements.** The support of the University of Bayreuth is gratefully acknowledged. We thank W. Joy and W. Reichstein for excellent technical assistance. We thank E. Penott-Chang, S. Graus-Molinero and A. H. E. Müller for the synthesis of the polymers.